

Electronic supplementary information

**Bio-catalytic nanoparticle shaping for preparing mesoscopic
assemblies of semiconductor quantum dots and organic molecules**

Rumana Akter¹, Nicholas Kirkwood², Samantha Zaman², Bang Lu^{1,3}, Tinci Wang¹, Satoru Takakusagi^{1,3}, Paul Mulvaney², Vasudevanpillai Biju^{1,4*}, Yuta Takano^{1,4*}

¹*Graduate School of Environmental Science, Hokkaido University, Sapporo 0600810, Japan*

²*ARC Centre of Excellence in Exciton Science, School of Chemistry, The University of Melbourne, Parkville, Victoria, 3010, Australia*

³*Institute for Catalysis, Hokkaido University, Sapporo 0010021, Japan*

⁴*Research Institute of Electronic Science, Hokkaido University, Sapporo 0010020, Japan*

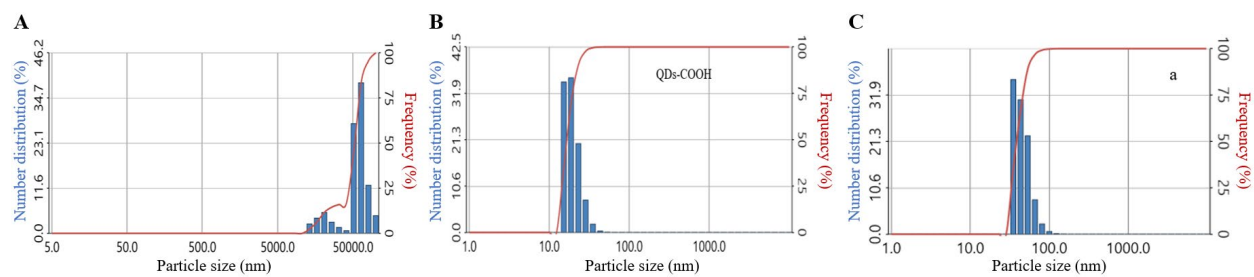


Fig. S1 DLS profiles of (A) a precipitate precursor for **ms-QD** before treating with trypsin, (B) **QD-COOH**, and (C) **ms-QD** in 10 mM HEPES aq.

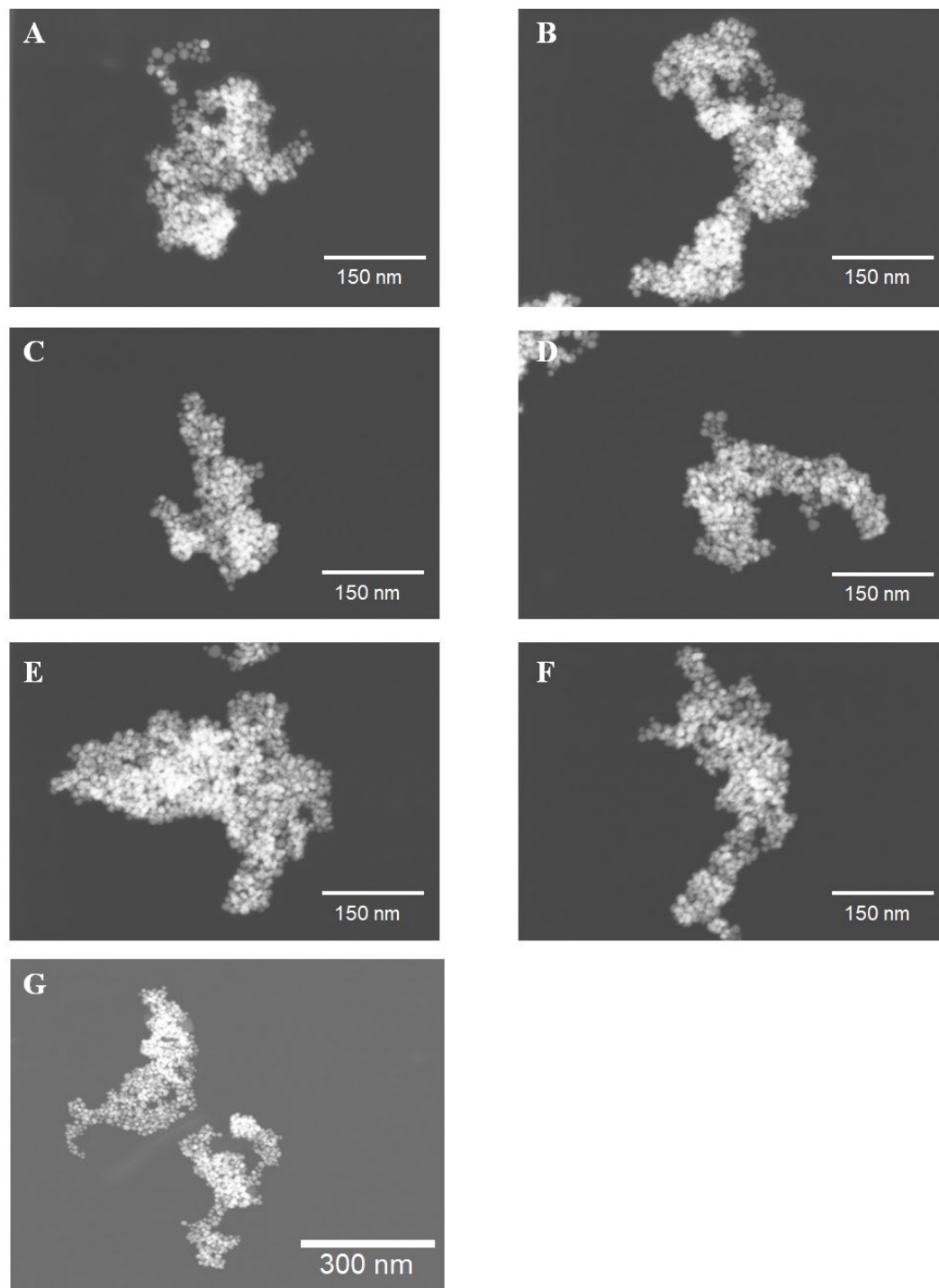


Fig. S2 Z-Contrast (ZC)-STEM mode images, which are derived from scattered electrons, of **ms-QD** (A-F) in different positions on the TEM grid and (G) the image shown in Fig. 1G in which the scale bar indicates 300 nm.

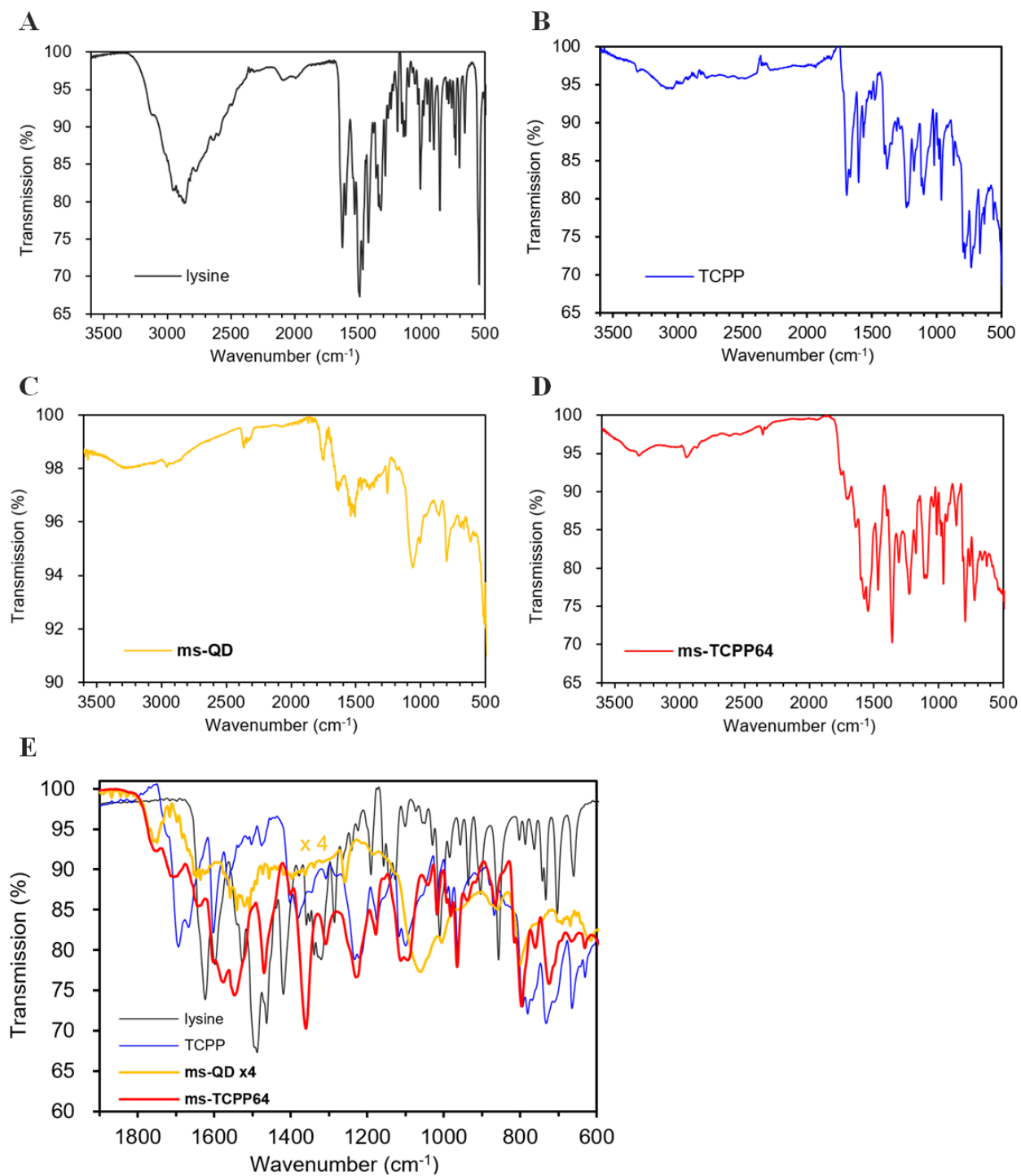


Fig. S3 FT-IR spectra of (A) L-lysine monohydrochloride, (B) TCPP, (C) **ms-QD** and (D) **ms-TCPP64**, and (E) their expanded spectra along with x-axis.

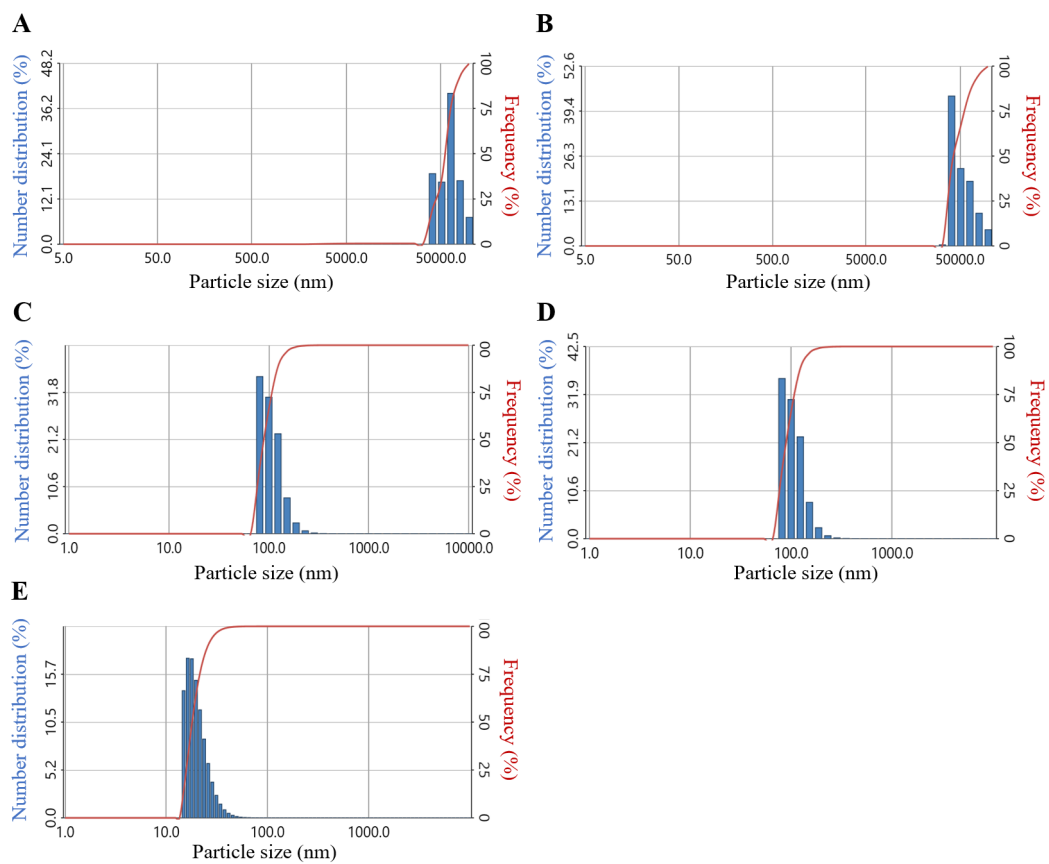


Fig. S4 DLS profiles of (A) mp-TCPP4, (B) mp-TCPP16, (C) mp-TCPP64, (D) mp-TCPP256 and (E) TCPP in 10 mM HEPES aq.

Table S1. The averaged hydrodynamic particle sizes with a standard deviation and poly-dispersibility index (PDI) obtained by the DLS measurements corresponding to Figure S2.

Compound	Averaged size (nm)	PDI
mp-TCPP4	>5000	n.a.
mp-TCPP16	>5000	n.a.
mp-TCPP64	106.2 ± 28.7	0.197
mp-TCPP254	100.9 ± 25.6	0.142
TCPP	20.3 ± 5.5	0.155

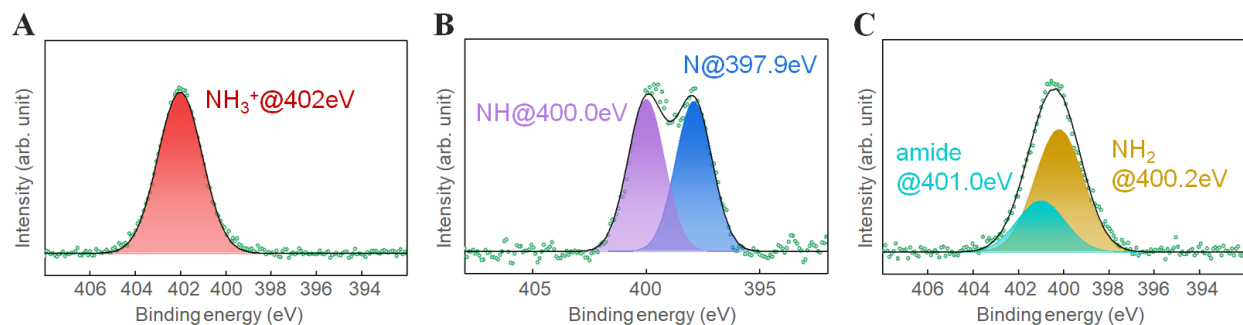


Fig. S5 X-ray photoelectron spectroscopy (XPS) data of (A) L-lysine hydrochloride, (B) TCPP, and (D) **ms-TCPP64**. L-lysine shows a dominant peak derived from NH_3^+ because it is a hydrochloride salt¹, while TCPP shows two characteristic peaks derived from the central unit of the porphyrin moiety.² **ms-TCPP64** demonstrates two characteristic peaks from the amide bonds and the amino moieties,¹ whereas the excess of the oligo-lysine moiety in ms-TCPP64 obscures the peaks seen in TCPP.

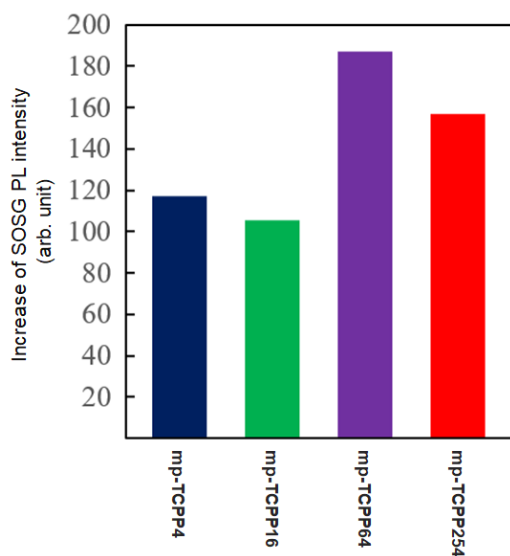


Fig. S6 $^1\text{O}_2$ generation ability assays using SOSG as the detecting reagent under an NIR light irradiation (Xe lamp, 700 ± 25 nm bandpass, 5 min, 50 mW/cm^2).

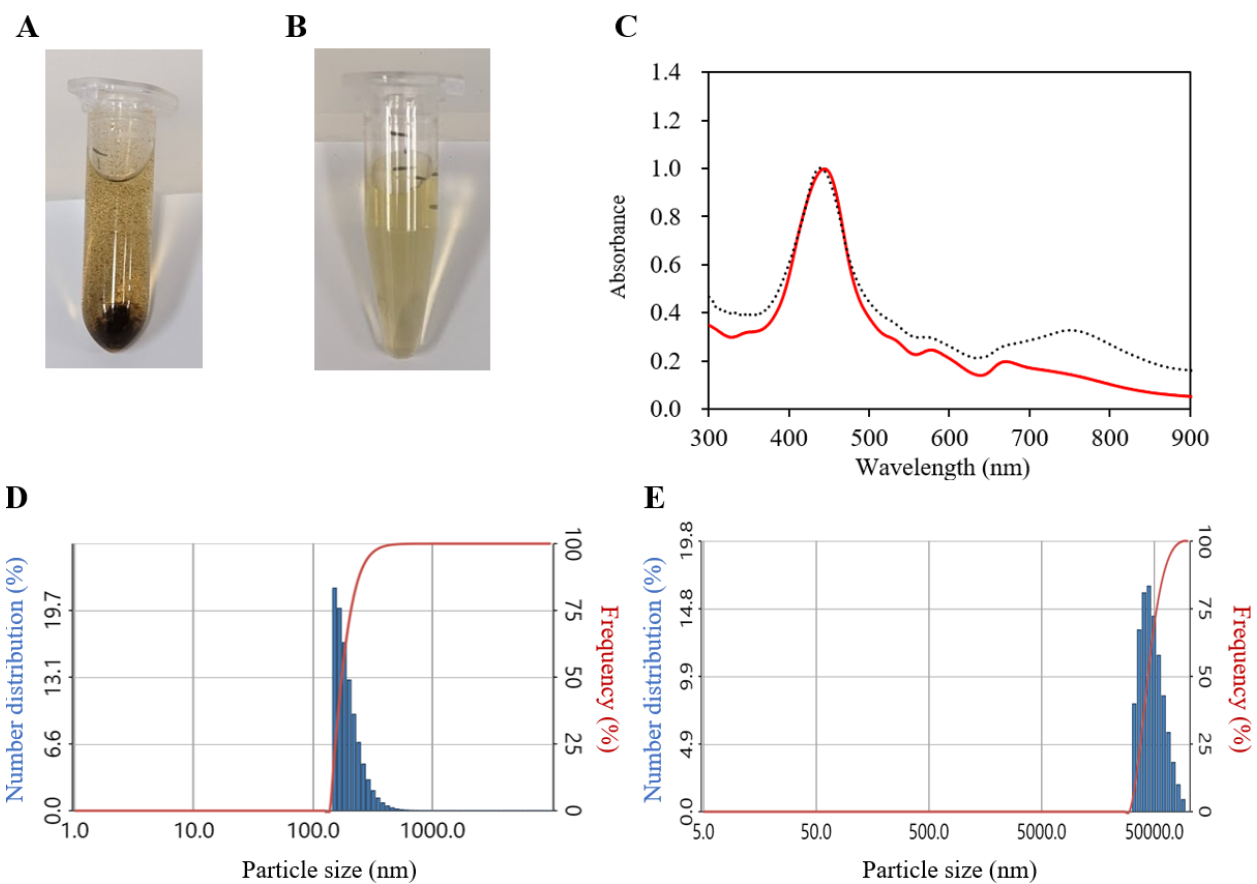


Fig. S7 Photo images of (A) the precipitate precursor and (B) the resultant **mp-TAPP/HA**. (C) Absorption spectra and (D) DLS profiles of **mp-TAPP/HA** in water. (E) DLS profiles of the precipitate precursor treated with trypsin instead of hyaluronidase.

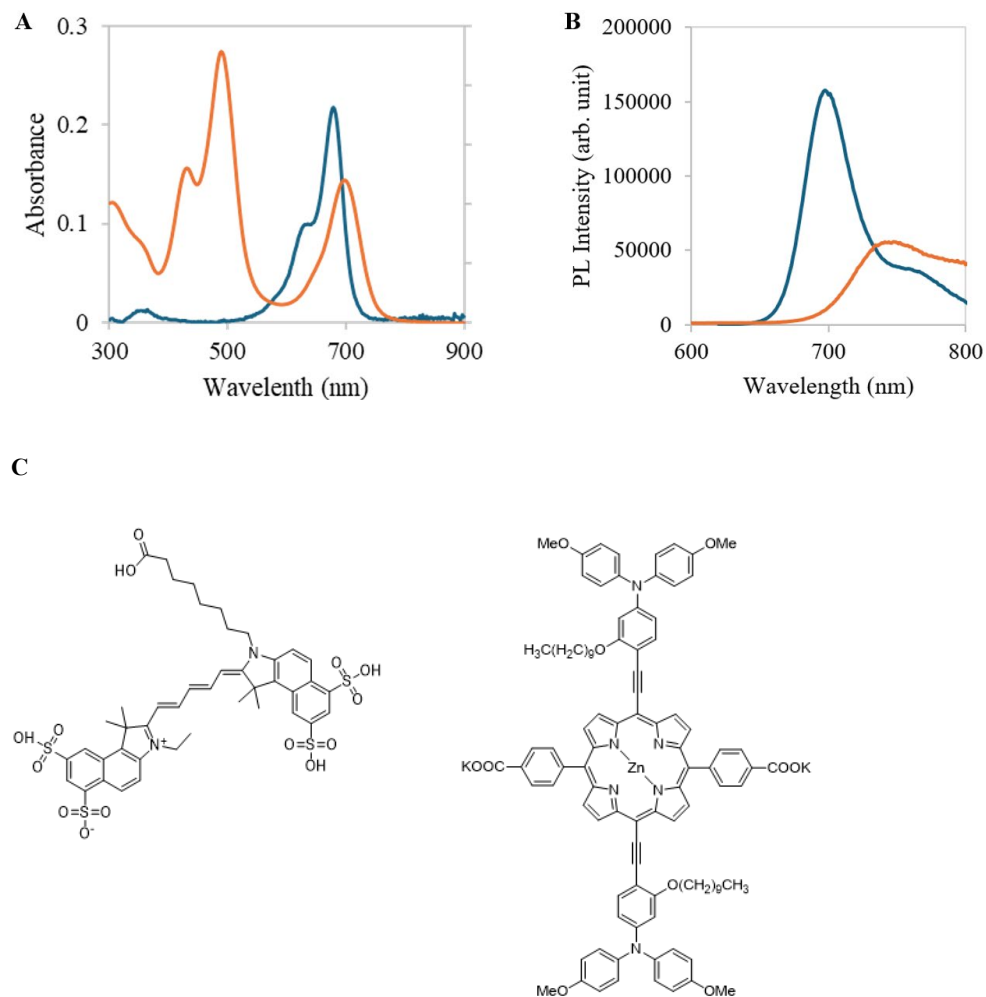


Fig. S8 (A) Absorption spectra of (blue) sulfo-Cy5.5 (orange) and **rTPA** and, (B) Photoluminescence spectra (λ_{ex} : 650 nm and 480 nm) of (blue) Sulfo Cy5.5 and (orange) **rTPA** in 10 mM HEPES aq. (C) The molecular structures of (left) sulfo-Cy5.5 and (right) **rTPA**

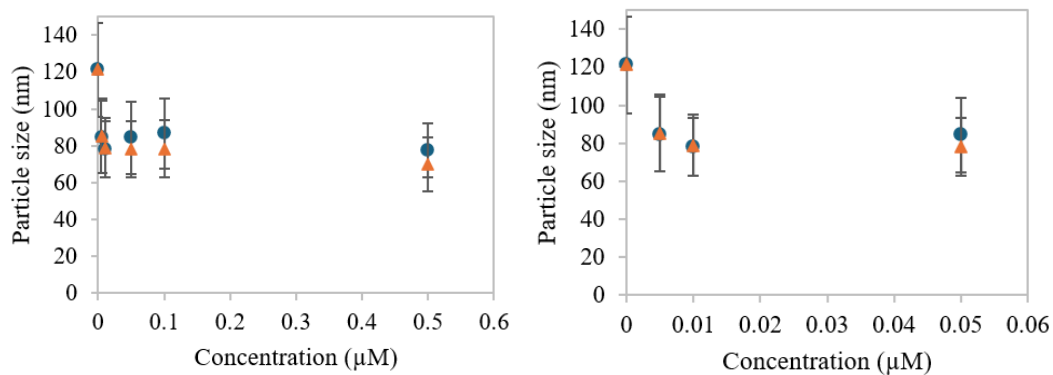


Fig. S9 (A) The averaged hydrodynamic particle sizes of **ms-QD** with an additive (blue circle: sulfo-Cy5.5, and orange triangle: **rTPA**) obtained by DLS measurements in 10 mM HEPES aq. (B) An expanded plot along with the x-axis. Error bars indicate a standard deviation.

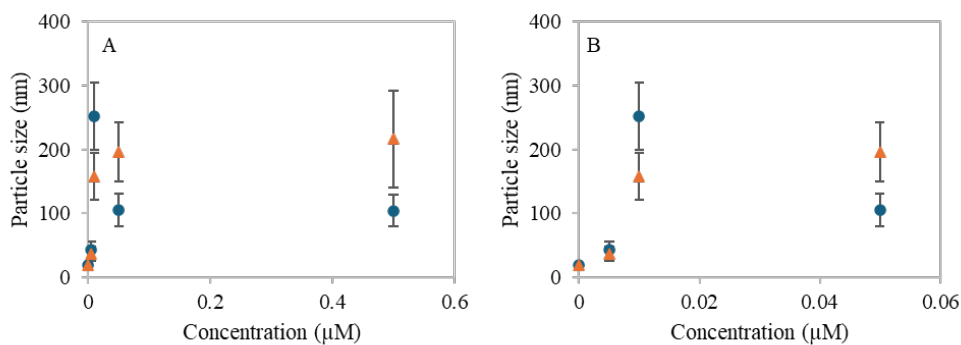


Fig. S10 (A) The averaged hydrodynamic particle sizes of **mono-QD** with an additive (blue circle: sulfo-Cy5.5, and orange triangle: **rTPA**) obtained by DLS measurements in 10 mM HEPES aq. (B) An expanded plot along with the x-axis. Error bars indicate a standard deviation. The large error bars indicate the size distributions are broad.

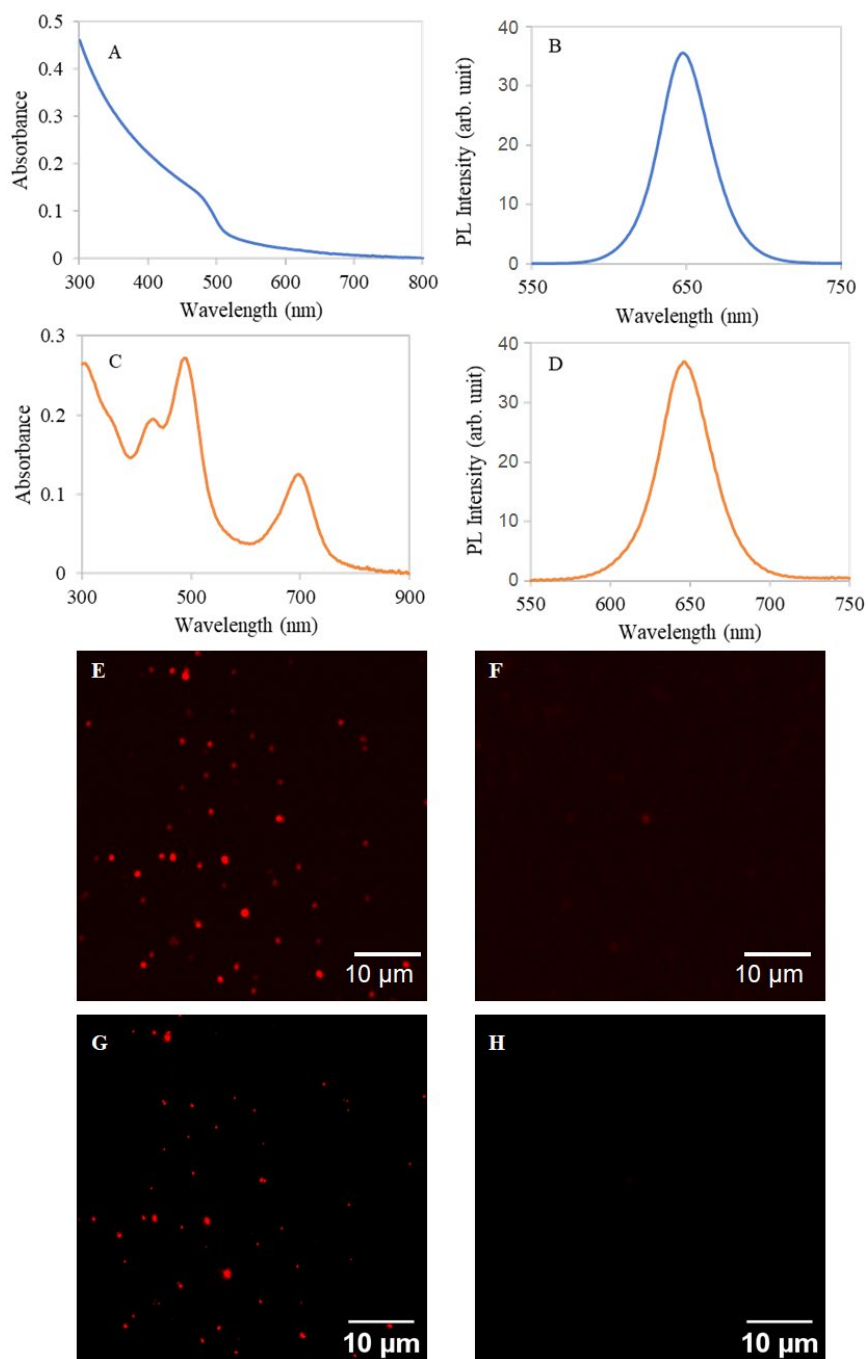


Fig. S11 Absorption spectra and photoluminescence spectra (λ_{ex} , 405 nm) of (A and B) **ms-QD** and (C and D) **rTPA@ms-QD** in 10 mM HEPES aq. Laser microscopic images of (E and G) **rTPA@ms-QD** and (F and H) **rTPA@mono-QD** on a glass coverslip under the identical excitation laser powers at (E and F) 800 nm *fs*-laser and (G and H) 405 nm CW laser with the identical detector sensitivity on the best focus.

References:

- 1 T. Eralp, A. Shavorskiy and G. Held, *Surf. Sci.*, 2011, **605**, 468–472.
- 2 W.-R. Cai, W.-K. Zhu, B.-Z. Yang, D.-T. Wu, J.-Y. Li, Z.-Z. Yin and Y. Kong, *Chemosensors*, 2022, **10**, 519.